ISSN 1674-1056
http://cpb.iphy.ac.cn
http://iopscience.iop.org/cpb
中国物理 B
Chinese Physics
中国物理 Chinese Physics B

Double band-inversions of bilayer phosphorene under strain and their effects on optical absorption

Shi He(何诗), Mou Yang(杨谋), Rui-Qiang Wang(王瑞强)
Citation: Chin. Phys. B . 2018, 27(4): 047303. **doi:** 10.1088/1674-1056/27/4/047303

Journal homepage: http://cpb.iphy.ac.cn; http://iopscience.iop.org/cpb

What follows is a list of articles you may be interested in

Conductivity and band alignment of $LaCrO_3/SrTiO_3$ (111) heterostructure

Yan-Peng Hong(洪彦鹏), Xin-Xin Wang(王欣欣), Guo-Liang Qu(曲国良), Cheng-Jian Li(厉承剑), Hong-Xia Xue(薛红霞), Ke-Jian Liu(刘科践), Yong-Chun Li(李永春), Chang-Min Xiong(熊昌民), Rui-Fen Dou(窦瑞芬), Lin He(何林), Jia-Cai Nie(聂家财)
Chin. Phys. B . 2018, 27(4): 047301. **doi:** 10.1088/1674-1056/27/4/047301

Van der Waals heterostructure of phosphorene and hexagonal boron nitride: First-principles modeling

Peng Zhang(张鹏), Jing Wang(王静), Xiang-Mei Duan(段香梅)
Chin. Phys. B . 2016, 25(3): 037302. **doi:** 10.1088/1674-1056/25/3/037302

Comparison of electronic structure between monolayer silicenes on Ag (111)

Chun-Liang Lin, Ryuichi Arafune, Maki Kawai, Noriaki Takagi
Chin. Phys. B . 2015, 24(8): 087307. **doi:** 10.1088/1674-1056/24/8/087307

Electronic structure of silicene

L. C. Lew Yan Voon
Chin. Phys. B . 2015, 24(8): 087309. **doi:** 10.1088/1674-1056/24/8/087309

Two-dimensional metallic behavior at polar $MgO/BaTiO_3$ (110) interfaces

Du Yan-Ling, Wang Chun-Lei, Li Ji-Chao, Zhang Xin-Hua, Wang Fu-Ning, Liu Jian, Zhu Yuan-Hu, Yin Na, Mei Liang-Mo
Chin. Phys. B . 2015, 24(3): 037301. **doi:** 10.1088/1674-1056/24/3/037301

Double band-inversions of bilayer phosphorene under strain and their effects on optical absorption*

Shi He(何诗), Mou Yang(杨谋)†, and Rui-Qiang Wang(王瑞强)

Guangdong Provincial Key Laboratory of Quantum Engineering and Quantum Materials, School of Physics and Telecommunication Engineering, South China Normal University, Guangzhou 510006, *China*

(Received 5 December 2017; revised manuscript received 16 January 2018; published online 29 March 2018)

Strain is a powerful tool to engineer the band structure of bilayer phosphorene. The band gap can be decreased by vertical tensile strain or in-plane compressive strain. At a critical strain, the gap is closed and the bilayer phosphorene is turn to be a semi-Dirac semimetal material. If the strain is stronger than the criterion, a band-inversion occurs and it re-happens when the strain is larger than another certain value. For the zigzag bilayer phosphorene ribbon, there are two edge band dispersions and each dispersion curve represents two degenerate edge bands. When the first band-inversion happens, one of the edge band dispersion disappears between the band-cross points while the other survives, and the latter will be eliminated between another pair of band-cross points of the second band-inversion. The optical absorption of bilayer phosphorene is highly polarized along armchair direction. When the strain is turn on, the optical absorption edge changes. The absorption rate for armchair polarized light is decreased by gap shrinking, while that for zigzag polarized light increases. The band-touch and band-inversion respectively result in the sublinear and linear of absorption curve versus light frequency in low frequency limit.

Keywords: phosphorene, electronic structure, optical absorption, strain

PACS: 73.22.–f, 73.23.–b, 78.20.–e **DOI:** 10.1088/1674-1056/27/4/047303

1. Introduction

Few layer black phosphorus, also called phosphorene, was exfoliated from its bulk black phosphorus recently.[1] Phosphorene is regarded as a very promising two-dimensional material due to its excellent electronic, mechanical, and optical properties. Phosphorene has very high mobility[2,3] and possesses a moderate band gap varying from 0.35 eV through 1.73 eV,[4] depending on the number of layers of phosphorene. It was demonstrated that the field-effect transistors of phosphorene have high on-off current ratio at room temperatures, which shows that phosphorene is a good candidate material for electronic application.[5–7] The energy gap is direct, which makes phosphorene become an alternative material that may detect the entire visible spectrum of light and near-infrared light region.[8,9] The band edge optical absorption is extreme anisotropic. Monolayer phosphorene absorbs the light polarized in the armchair direction while cannot take in that polarized along the zigzag direction.[10,11]

Phosphorene is a superior flexible material owing to its puckered honeycomb-like lattice and can sustain strong strain up to 30%,[12,13] which provides the probability to adjust its strain-sensitive properties by exerting strain on the phosphorene sheet. The energy gap as well as the effective mass can be controlled by strain, and this suggests phosphorene has a great potential for switching device fabrication.[11,14,15] Recent literatures reported that strain can tune the band structure of monolayer phosphorene and can turn it to be a semi-Dirac semimetal material when the energy gap is closed.[11,15–17] However, the strain effect on few-layer phosphorene has not been explored yet. The response of multilayer material to external parameters is not always similar as that of its monolayer counterpart. For example, under vertical electric field, the energy gap is enlarged by vertical electric field for monolayer phosphorene[18] while it is narrowed for bilayer phosphorene.[19,20] Whether or not the strain results in the same effects for mono- and multilayer phosphorene needs to be checked carefully. For this reason, we study the electronic structure and optical absorption of bilayer phosphorene under the influence of strain using the tight-binding model. Either vertical tensile strain or an in-plane compressive strain reduces the band gap and the former is the more effective to modify the energy gap. If the applied strain exceeds the critical value for gap closing, a band-inversion happens. For the strain stronger than another certain value, a new band-inversion takes place. Zigzag bilayer phosphorene ribbon hosts two dispersion curves of edge bands in the whole Brillouin zone, while armchair one does not. The interval in k-space where the edge bands exist can be changed by strain. If the strain is applied so as to the first band-inversion occurs, one of the edge band dispersions is eliminated between the band-cross points but the other remains in the whole Brillouin zone. When the second band-inversion happens, the remained edge band dispersion disappears between the second

*Project supported by the National Natural Science Foundation of China (Grant Nos. 11774100 and 11474106).

†Corresponding author. E-mail: yang.mou@hotmail.com

© 2018 Chinese Physical Society and IOP Publishing Ltd

pair of band-cross points. These features of bilayer phosphorene are all qualitative explained based on the band structure of monolayer phosphorene and the interlayer coupling. The optical absorption is almost completely polarized along armchair direction, and the polarization is weakened by gap shrinking. The absorption edges lead to triangle steps on the absorption curve versus frequency for the armchair polarized light. The triangle steps disappear when bands touch, and they evolve into sharp peaks if the band-inversion happens.

2. Electronic structure

2.1. Bulk material

The lattice structure of bilayer phosphorene is shown in Fig. 1. The vectors $\boldsymbol{a}$, $\boldsymbol{b}$, and $\boldsymbol{l}$ are used to reflect the geometry of phosphorene lattice and their components are listed in Table 1. The tight-binding Hamiltonian reads

$$H = \sum_{i,j} t_{ij} c_i^{\dagger} c_j, \tag{1}$$

where the summation runs over all of the lattice sites, $c_i^{\dagger}$ (c_i) is the electron creation (annihilation) operator on site i, and t_{ij} is the hopping energy between sites i and j. A recent literature reported that, when taking into account ten types of intra-layer hoppings ($t_1 \sim t_{10}$) and five types of inter-layer ones ($s_1 \sim s_5$), the electronic structure obtained by using the tight-binding model and that calculated from *ab initio* method coincide with each other perfectly[19,20] and the energy gap is quite close to the value measured experimentally.[4] The fifteen nonzero hoppings are marked in Fig. 1 and their values are listed in Table 2.

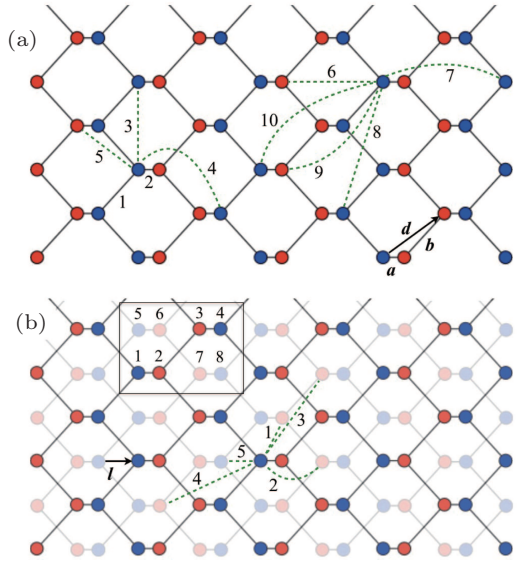


Fig. 1. (color online) (a) Monolayer phosphorene lattice and ten types of intra-layer hoppings. (b) Bilayer phosphorene lattice and five types of inter-layer hoppings. The red- and blue-filled circles denote puckered-up and puckered-down phosphorus atoms, the solid and semitransparent meshes represent the upper and lower phosphoene layer respectively, and the rectangle shows the unit cell.

Table 1. Geometry parameters without strain[19,20] (in unit Å).

	$\boldsymbol{a}$	$\boldsymbol{b}$	$\boldsymbol{l}$
x	0.7053	1.4797	1.4797
y	0	1.6550	0
z	2.1261	0	5.2349

Table 2. Hopping energies without strain[19,20] (in unit eV).

t_1	t_2	t_3	t_4	t_5
−1.486	3.729	−0.252	−0.071	0.0019
t_6	t_7	t_8	t_9	t_{10}
0.186	−0.063	0.101	−0.042	0.073
s_1	s_2	s_3	s_4	s_5
0.524	0.180	−0.123	−0.168	0.005

When a strain is applied on the lattice along the axes, the change of bonds can be described by

$$\boldsymbol{r}_{ij} = (1+\boldsymbol{\epsilon}) \cdot \boldsymbol{r}_{ij}^0, \tag{2}$$

where $\boldsymbol{\epsilon} = (\epsilon_x, \epsilon_y, \epsilon_z)$ is the strain with ε_α being the strain component along α direction, $\boldsymbol{r}_{ij}$ is the position vector originated from site i pointing to site j, and $\boldsymbol{r}_{ij}^0$ means $\boldsymbol{r}_{ij}$ at $\boldsymbol{\epsilon} = 0$. When the lattice is deformed, both the bond length and the bond angle are changed, and the modification of either ones alters the corresponding hopping energy. A popular approximation is that the hopping energy depends only on the bond length as[22,23]

$$\frac{t_{ij}}{t_{ij}^0} = \left(\frac{r_{ij}}{r_{ij}^0} \right)^{-2}, \tag{3}$$

where t_{ij}^0 denotes t_{ij} without strain.

Choosing a translational cell and labeling the eight atoms in it by 1 through 8 (see Fig. 1), we have the spinless Hamiltonian in k-space

$$H = \begin{pmatrix} H_{\mathrm{M}} & H_{\mathrm{C}} \\ H_{\mathrm{C}}^{+} & H_{\mathrm{M}} \end{pmatrix}, \tag{4}$$

where H_{M} is the Hamiltonian of monolayer phosphorene and H_{C} is the coupling between the two phosphorene layers. The monolayer Hamiltonian is defined by

$$H_{\mathrm{M}} = \begin{pmatrix} h_{11} & h_{12} & h_{13} & h_{14} \\ & h_{11} & h_{14}^* & h_{13} \\ & & h_{11} & h_{12} \\ & & & h_{11} \end{pmatrix}, \tag{5}$$

in which the lower triangular elements are not shown and they can be easily recovered by means of the hermitian of the matrix. The inter-layer Hamiltonian reads

$$H_{\mathrm{C}} = \begin{pmatrix} 0 & h_{16} & h_{17} & h_{18} \\ & 0 & & \\ & & 0 & \\ h_{18}^* & h_{17}^* & h_{16}^* & 0 \end{pmatrix}.$$

The matrix elements in the two matrices are calculated to be

$$
\begin{aligned}
h_{11} &= 2t_3\cos 2k_y d_y + 2t_7\cos 2k_x d_x + 4t_{10}\cos 2k_x d_x \cos 2k_y d_y,\\
h_{12} &= t_2\,\mathrm{e}^{\mathrm{i}k_x a_x} + t_6 e^{-ik_x(d_x+b_x)} + 2t_9\,\mathrm{e}^{-\mathrm{i}k_x(d_x+b_x)}\cos 2k_y d_y,\\
h_{13} &= 4t_5\cos k_x d_x \cos k_y d_y,\\
h_{14} &= 2t_1\,\mathrm{e}^{-\mathrm{i}k_x b_x}\cos k_y d_y + 2t_4\,\mathrm{e}^{\mathrm{i}k_x(d_x+a_x)}\cos k_y d_y\\
&\quad + 2t_8\,\mathrm{e}^{-\mathrm{i}k_x b_x}\cos 3k_y d_y,\\
h_{16} &= 2s_1\,\mathrm{e}^{-\mathrm{i}k_x a_x}\cos k_y d_y + 2s_4\,\mathrm{e}^{-\mathrm{i}k_x(d_x+b_x)}\cos k_y d_y,\\
h_{17} &= 4s_3\cos k_x d_x \cos 2k_y d_y + 2s_2\cos k_x d_x,\\
h_{18} &= s_5\,\mathrm{e}^{-\mathrm{i}k_x b_x},
\end{aligned}
\tag{6}
$$

where d_x and d_y are the components of vector $\boldsymbol{d}=\boldsymbol{a}+\boldsymbol{b}$, which are adopted to simplify the notations.

Before we diagonalize the Hamiltonian matrix to obtain the band structure, we analyse the bilayer system quantitatively to have some basic features without detailed calculations. A unit cell contains eight atoms, so that there are eight bands in total. Two highest bands and two lowest bands are much far away from the energy gap, and they are not considered in the following. Only four bands, two conduction and two valence bands that are close to the energy gap, are involved into our calculation and discussions. Because the coupling between layers is much weaker than the intra-layer hoppings, the bilayer system can be viewed as two monolayers perturbed by the inter-layer coupling. The energy dispersions of the two monolayers without coupling are degenerate. If turning on the inter-layer coupling, the degeneracy is lifted. Supposing the energy split for the conduction or valence band at the wavevector $\boldsymbol{k}$ to be $2\Delta_\alpha(\boldsymbol{k})$ $(\alpha = c, v)$, we have the energy bands of bilayer phosphorene

$$E_\alpha^{\pm} = \varepsilon_\alpha \pm \Delta_\alpha, \tag{7}$$

where ε is the energy dispersion of monolayer phosphorene. Therefore, we have the bands of the bilayer phosphorene based on those of monolayer phosphorene and the inter-layer coupling.

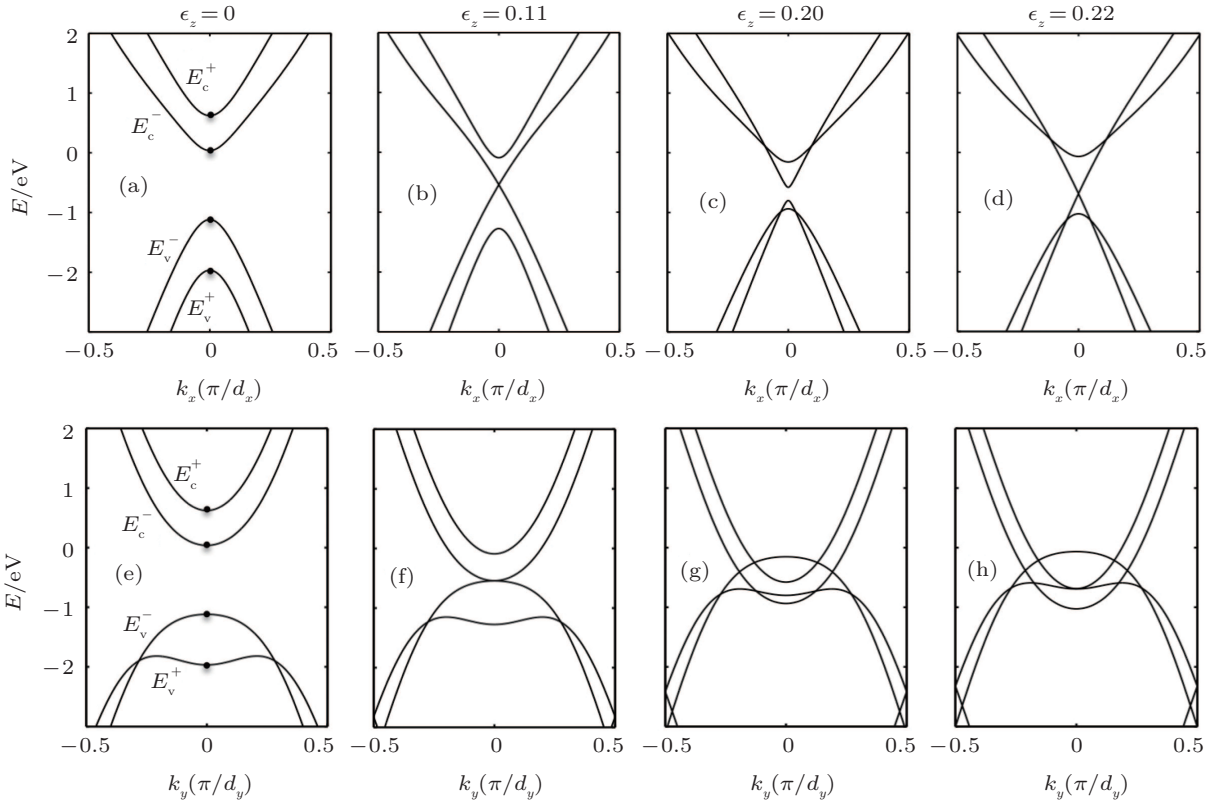


Fig. 2. Energy bands along the lines $k_y = 0$ [panels (a)–(d)] and $k_x = 0$ [panels (e)–(h)] for differen values of ϵ_z.

Figure 2 shows the energy bands of bilayer phosphorene under different strains along the z direction. One can see that the two valence bands intersect with each other. This is because the split Δ chances its sign at some wavevectors. For the strainless case, the signs of Δ of the conduction and valence bands are opposite at Γ point. We divide the four bands into two conduction-valence band pairs $(E_{\mathrm{c}}^+, E_{\mathrm{v}}^+)$ and $(E_{\mathrm{c}}^-, E_{\mathrm{v}}^-)$. The gap of the latter pair is smaller than that of the former pair and is the band gap of bilayer system. When the lattice is strained, the energy bands move and the energy gap varies. The band gap is decreased by applying tensile strain and at the critical value $\epsilon_z = 0.11$, the conduction and valence bands of the band pair $(E_{\mathrm{c}}^-, E_{\mathrm{v}}^-)$ touch each other and the band gap is completely closed. At this situation, the dispersion in x (armchair) direction is linear and is parabolic in y (zigzag) direction, and the bilayer phosphorene becomes a semi-Dirac

semimetal material. A band-inversion occurs if the strain becomes stronger, and the two band-cross points serve like the Dirac points in graphene. At a certain larger value of strain, saying, $\epsilon_z = 0.22$, another conduction-valence band pair touch each other, and the second band-inversion will take place for larger strains. The band-inversions play important role for topological phase transition, that will be explained later.

Figure 3(a) shows the energy gap at Γ point as a function of uniaxial strains along x, y, and z directions. The energy gap can be decreased by in-plane compressive strain as well as by vertical tensile strain. At the in-plane critical strain $\epsilon_x = -0.28$ or $\epsilon_y = -0.17$, the band-close happens. Among the three strain components, the band structure is most sensitive to the vertical strain. Between the first and the second band-touch cases, there are plateaus on the energy gap curves. Because the positive strain in z direction and the negative strains along in-plane directions have qualitatively similar effects on the band structure, we will only discuss former case from here on. Figure 3(b) shows the curves of band energies at Γ point (these energies are marked by the bold dots in Fig. 2) versus strain along z direction. One can find that the plateaus on the energy gap curves are caused by the intersections between the band energy curves belong to different conduction–valence band pairs, as indicated by the vertical dashed lines in Fig. 3.

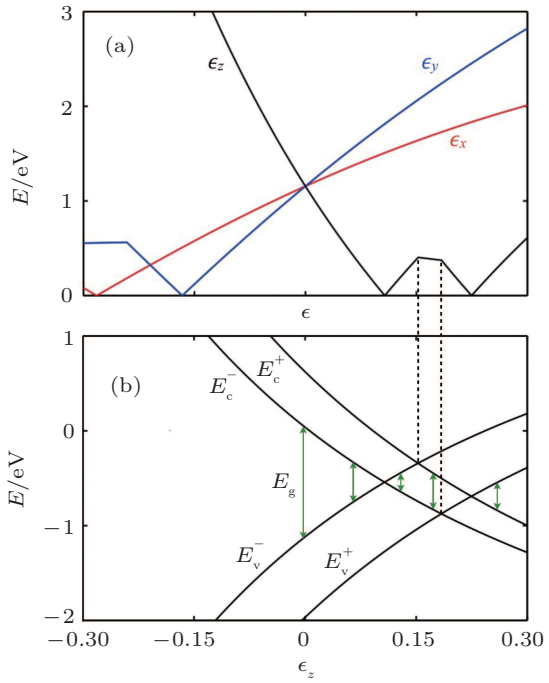


Fig. 3. (color online) (a) The energy gap at Γ point as a function of uniaxial strains. (b) The band energies at Γ point versus ϵ_z.

2.2. Ribbons

Phosphorene ribbons have various types of edges, and some types of edges can accommodate edge bands.[24–26] To understand the edge bands of bilayer phosphorene ribbons, we first review the band structure of monolayer ones. For the zigzag ribbon, there exist two degenerate edge bands laying within the energy gap, while no edge band exists in the spectrum of the armchair ribbon. The quantum states belong to two edge bands are localized near the two opposite edges respectively, and the localization length of the edge states can be tuned by normally applied electric field.[26] If applying vertical tensile or compressive in-plane strain, the band gap shrinks. When the band gap is eliminated, the edge band dispersion comes across the band-touch point. For stronger strains, the band-inversion happens, the edge band dispersion joints with the bulk bands at the band-cross points, and no edge band can be found between the band-cross points. The above statements about the edge bands can be verified by the winding number analysis as reported in Refs. [24] and [25].

The edge bands of bilayer phosphorene can also be understood by means of the perturbation of the inter-layer coupling. If no coupling exists, the edge bands for the upper monolayer and those for the lower one are degenerate. When the coupling is turn on, the degeneracy is lifted. Denoting the edge band dispersion of monolayer as $\varepsilon_{\rm ed}$ and supposing the splitting of degeneracy broken to be $2\Delta_{\rm ed}$, we have two edge band dispersions for the bilayer phosphorene

$$E_{\rm ed}^{\pm} = \varepsilon_{\rm ed} \pm \Delta_{\rm ed}. \tag{8}$$

In the above equation, each edge band dispersion is still twofold degenerate, since the inter-layer coupling does not mix the edge states on different edges. Therefore, there are two edge band dispersions while four edge bands in a zigzag bilayer phosphorene ribbon.

Figure 4 shows the band structure of armchair and zigzag bilayer phosphorene ribbons. Because $\Delta_{\rm ed}$ changes its sign when the wavevector varies, the two edge bands curves for $E_{\rm ed}^+$ and $E_{\rm ed}^-$ cross each other. When the strain exceeds the critical value, the band-inversion of band-pair $(E_{\rm c}^-, E_{\rm v}^-)$ leads to the disappearing of edge band dispersion $E_{\rm ed}^-$ between the band-cross points, while the other edge band dispersion survives in the interval. If the strain is larger and the band-inversion of $(E_{\rm c}^+, E_{\rm v}^+)$ happens, the edge states of $E_{\rm ed}^+$ will be eliminated between the band-cross points of the second band-inversion.

One can find the edge band splitting when the band-touch happens, as shown in Figs. 4(f) and 4(h). The quantum states of the edge bands are localized near the edges. The decay length of the edge band states depends on the energy difference between these states and the bulk band states. When the band-touch happens, the decay length of the edge states near Γ point becomes very large and the edge states of the opposite edges overlap with each other. The non-negligible overlap results in a small splitting. The splitting is an effect of the finite width. If we use wider ribbons to calculate, the splitting will be less notable, and it will be invisible in the large width limit.

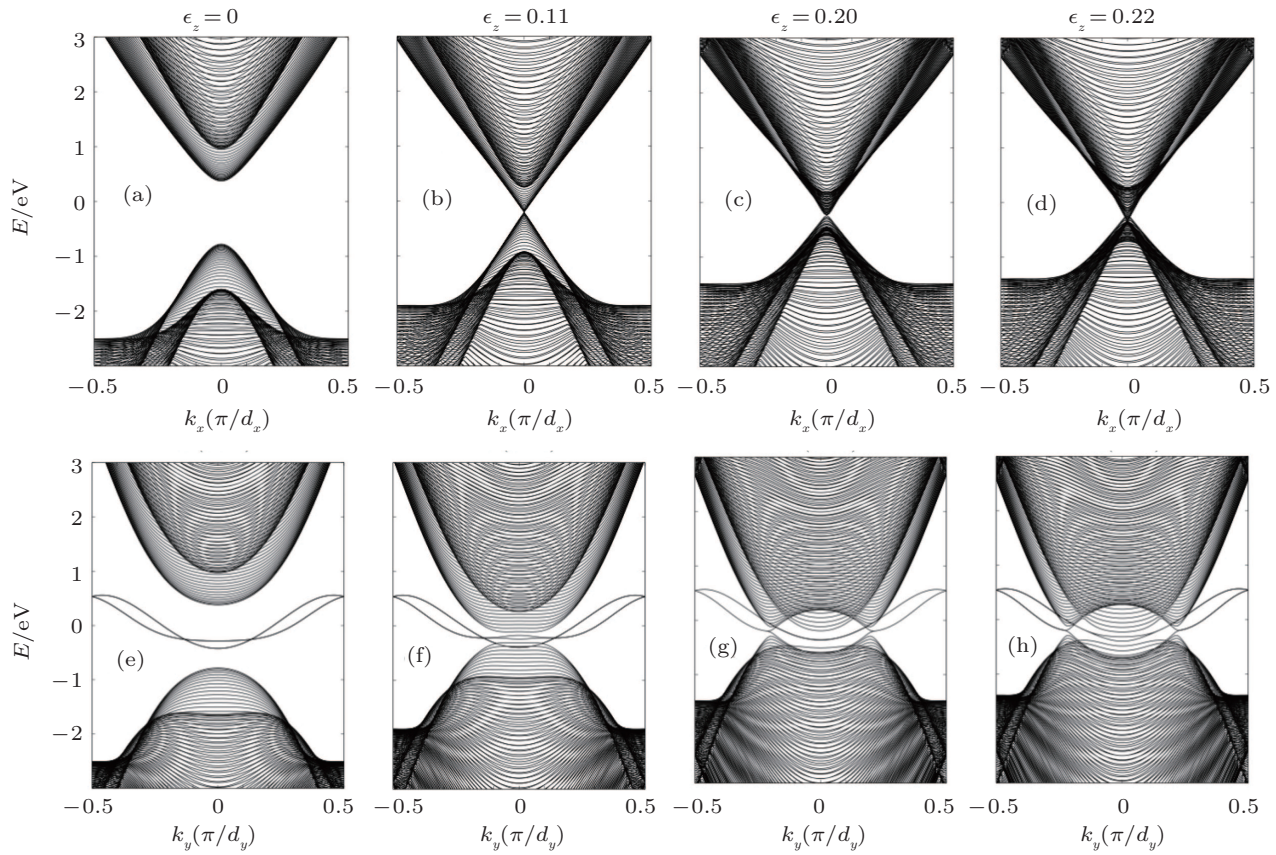


Fig. 4. Band structure of armchair-edged [panels (a)–(d)] and zigzag-edged [panels (e)–(h)] bilayer phosphorene ribbons for different values of ϵ_z. The number of unit cells in lateral direction is 50 for both armchair and zigzag ribbons.

3. Optical absorption

We consider that a polarized light with the angular frequency ω irradiates normally on a bulk bilayer phosphorene sheet. The light can be modeled by its time-dependent vector potential $\boldsymbol{A}e^{i\omega\tau}$, where $\boldsymbol{A} = (A_x, A_y)$ is the vector potential amplitude and τ is the time. The vector potential can be involved into the perturbation Hamiltonian by the so-called $A \cdot p$ approximation. Under the irradiation, the valence band electrons have the probability to be resonantly excited to the conduction band if the condition $E_c - E_v = \hbar\omega$ is satisfied, where $\hbar$ is the reduced Planck constant. By means of the standard time-dependent perturbation theory, the absorption rate (number of photons absorbed per unit time) at zero temperature is calculated by[18]

$$I(\omega) = \frac{e^2}{2\pi\hbar} \oint_{E_c - E_v = \hbar\omega} |\boldsymbol{A} \cdot \boldsymbol{P}|^2 \frac{\mathrm{d}\boldsymbol{k}}{\nabla_{\boldsymbol{k}}(E_c - E_v)}, \tag{9}$$

where e is the electron charge. In the equation, the vector $\boldsymbol{P} = (P_x, P_y)$ is defined by

$$\boldsymbol{P} = \langle \psi_c | \boldsymbol{v} | \psi_v \rangle. \tag{10}$$

In Eq. (10), ψ_c and ψ_v are the conduction and valence band states corresponding to the band energies E_c and E_v respectively, and $\boldsymbol{v}$ is the velocity operator defined as

$$\boldsymbol{v} = \frac{1}{\hbar} \nabla_k H. \tag{11}$$

First, we discuss the the optical absorption without strain. From here on, we set $|\boldsymbol{A}|$ to be constant and consider the polarization along x (armchair) or y (zigzag) direction. Figure 5(a) illustrates the absorption rate as function of photon energy. The absorption is nonzero when the photon energy larger than the band gap. The absorption curve of the x-polarized light shows two triangle steps, which reflect the two absorption edges $E_c^- - E_v^-$ and $E_c^+ - E_v^+$. While for the light polarized in the y direction, the absorption is quite small and increases monotonously with $\hbar\omega$. Thus, in the vicinity of the first absorption edge $E_c^- - E_v^-$, the absorption is totally polarized along the armchair direction.

Second, we turn on the strain ϵ_z and gradually enhance it to observe the absorption property. Figures 5(b) through 5(d) show the absorption rate versus photon energy under different strains. The strain response of absorption of the x-polarized light and that of the y-polarized light are quite different. For the x-polarized light, the two absorption edges are decreased by the strain, and thus the two triangle steps shift to the left end. When the bands of E_v^- and E_c^- touch, the first absorption edge vanishes, and the absorption rate dives to zero sublinearly, that reflects the property of joint state density of semi-Dirac semi-parabolic dispersion. When the strain exceeds the criterion strain and the first band-inversion happens, the absorption curve becomes linear near the left end, that is the sig-

nal of the joint state density for the Dirac type dispersion. A sharp peak on the curve can be found under this situation, and it is attributed by the inverse band gap. If the second band-pair touch, the second absorption peak disappears. When the strain is enough large so as to the second band-inversion appears (not shown in the figure), a new sharp peak will take place. The above statements can be well described phenomenally as follows. When the strain increase continuously, the triangle peaks of the absorption edge move left and lower down, and disappear when they arrive at the vertical axis ($\hbar\omega = 0$); after they hit the axis, they are reflected, revived as sharp peaks and propagate back. For the light polarized along the y direction, the absorption is quite simple. The gap shrink leads to the absorption edge changes, and the absorption rate increases with the applied strain ϵ_z.

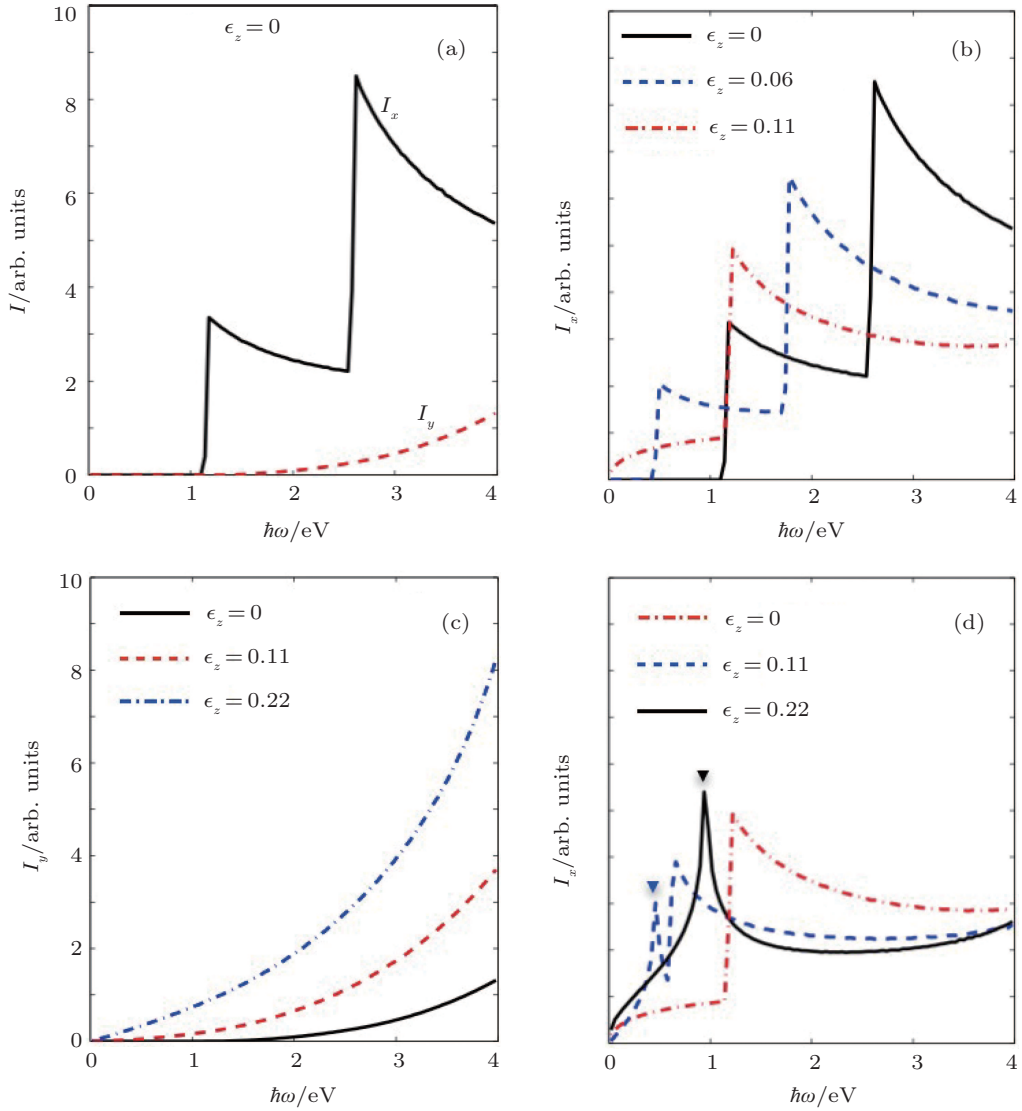


Fig. 5. (color online) The optical absorption rate of bilayer phosphorene as function of photon energy. (a) The absorption without strain, (b) and (d) the absorption of x-polarized light under different ϵ_z, (c) the absorption of y-polarized light under different ϵ_z. The triangle symbols is used to label the sharp peaks of inverse band gaps.

4. Summary

The electronic structure of bilayer phosphorene can be tuned by strain engineering. Applying a vertical tensile strain or an in-plane strain can decrease the band gap. At the critical strain to vanish the band gap, the bilayer phosphorene becomes a semi-Dirac semimetal material. The band-inversion happens under larger strain. At another certain strain, a new band-touch takes place and the second band-inversion will take place if the strain is increased. Each edge of the zigzag bilayer phosphorene ribbon accommodates two non-degenerate edge band curves in the whole Brillouin zone for the strainless case. If the strain is applied so as to the band-inversion happens, the two edge band curves are eliminated between the band-cross points of the first band-inversion and the second one respectively. The optical absorption of bilayer phosphorene is highly polarized along the armchair direction without strain, while the polarization is notablely weakened for strain-induced band-touch and band-inversion cases. When the gap shrinks, the absorption rate for armchair polarized light or

zigzag polarized light decreases or increases respectively. The absorption as function of light frequency is sublinear in the low frequency region if the band-touch happens, and it is linear for the band-inversion cases.

References

[1] Xia F, Wang H and Jia Y 2014 *Nat. Commun.* **5** 4458
[2] Liu H, Neal A T, Zhu Z, Luo Z, Xu X, Tománek D and Ye P D 2014 *ACS Nano* **8** 4033
[3] Rudenko A N, Brener S and Katsnelson M I 2016 *Phys. Rev. Lett.* **116** 246401
[4] Li L, Kim J, Jin C, Ye G, Qiu D. Y, da Jornada F H, Shi Z, Chen L, Zhang Z, Yang F, Watanabe K, Taniguchi T, Ren W, Louie S G, Chen X, Zhang Y and Wang F 2017 *Nat. Nanotechnol.* **12** 21
[5] Li L, Yu Y, Ye G J, Ge Q, Ou X, Wu H, Feng D, Chen X H and Zhang Y 2014 *Nat. Nanotechnol.* **9** 372
[6] Koenig S P, Doganov R A, Schmidt H, Neto A H and Özyilmaz B 2014 *Appl. Phys. Lett.* **104** 103106
[7] Yin D and Yoon Y 2016 *J. Appl. Phys.* **119** 214312
[8] Youngblood N, Chen C, Koester S J and Li M 2015 *Nat. Photon.* **9** 247
[9] Buscema M, Groenendijk D J, Blanter S I, Steele G A, van der Zant H S J and Castellanos-Gomez A 2014 *Nano Lett.* **14** 3347
[10] Tran V, Soklaski R, Liang Y and Yang L 2014 *Phys. Rev. B* **89** 235319
[11] Duan H J, Yang M and Wang R Q 2016 *Physica E* **81** 177
[12] Wei Q and Peng X 2014 *Appl. Phys. Lett.* **104** 251915
[13] Peng X, Wei Q and Copple A 2014 *Phys. Rev. B* **90** 085402
[14] Han X, Stewart H M, Shevlin S A, Richard C, Catlow A and Guo Z X 2014 *Nano Lett.* **14** 4607
[15] Jiang J W and Park H S 2015 *Phys. Rev. B* **91** 235118
[16] Elahi M, Khaliji K, Tabatabaei S M, Pourfath M and Asgari R 2015 *Phys. Rev. B* **91** 115412
[17] Sisakht E T, Fazileh F, Zare M H, Zarenia M and Peeters F M 2016 *Phys. Rev. B* **94** 085417
[18] Yang M, Duan H J and Wang R Q 2016 *Phys. Scr.* **91** 105801
[19] Rudenko A N, Yuan S and Katsnelson M I 2015 *Phys. Rev. B* **92** 085419
[20] Kim J, Baik S S, Ryu S H, Sohn Y, Park S, Park B G, Denlinger J, Yi Y, Choi H J and Kim K S 2015 *Science* **349** 723
[21] Rudenko A N, Yuan S and Katsnelson M I 2016 *Phys. Rev. B* **93** 199906
[22] Harrison W A 1999 *Elementary Electronic Structure* (Singapore: World Scientific)
[23] Tang H, Jiang J W, Wang B S and Su Z B 2009 *Solid State Commun.* **149** 82
[24] Ezawa M 2014 *New J. Phys.* **16** 115004
[25] Yang M, Duan H J and Wang R Q 2015 *JETP Lett.* **102** 610
[26] Yang M, Duan H J, He S, Zhang W L and Wang R Q 2016 *Phys. Lett. A* **380** 3832